The Cryosphere Discuss., 4, 2337–2372, 2010
www.the-cryosphere-discuss.net/4/2337/2010/
doi:10.5194/tcd-4-2337-2010

The Cryosphere Discussions

Retrieval of snow albedo and grain size using reflectance measurements in Himalayan basin

H. S. Negi[1,2] and A. Kokhanovsky[2]

[1]Snow & Avalanche Study Establishment, Him Parisar, Sector-37A, Chandigarh 160 036, India
[2]Institute of Environmental Physics, University of Bremen, O. Hahn Allee 1, 28359 Bremen, Germany

Received: 18 October 2010 – Accepted: 22 October 2010 – Published: 4 November 2010

Correspondence to: H. S. Negi (negi_hs@yahoo.com)

Published by Copernicus Publications on behalf of the European Geosciences Union.

Abstract

In the present paper spectral reflectance measurements of Himalayan seasonal snow were carried out and analysed to retrieve the snow albedo and effective grain size. The asymptotic radiative transfer (ART) theory was applied to retrieve the plane and spherical albedo. The retrieved plane albedo was compared with the measured spectral albedo and a good agreement was observed with ±10% measured error accuracy. Retrieved integrated albedo was found within ±6% difference with ground observed broadband albedo. The snow grain sizes retrieved using different models based on ART theory are compared for different snow types and it was observed that presently grain size model using two channel method (one in visible and another in NIR region) can work well for Himalayan seasonal snow and it was found consistence with temporal increased grain size. This method can work very well for clean dry snow like in upper Himalaya but sometime due to low reflectances (<0.2) using wavelength 1.24 µm ART theory can not be applied, which is common in lower and middle Himalayan old snow. This study is of importance for monitoring the Himalayan cryosphere using air-borne or space-borne sensors.

1 Introduction

Snow is an important natural resource. Due to high albedo of snow and its large areal extent on the terrestrial surface it has significant effects on the planetary climate. The snow albedo also influences the rate of melting and thus it is an important factor for the various activities related to seasonal snowcover. Therefore many studies have been carried out on albedo measurement and mapping the snow cover. The snow grain size and the impurities in snow are known as very important factors for changing the snow albedo (Wiscombe and Warren, 1980; Warren and Wiscombe, 1980; Aoki et al., 2003).

The Himalayan cryosphere has its importance because the presence of snow cover in Himalaya is due to its high elevations unlike the polar regions and the source of origin for many rivers. The vast area of Himalaya receives snowfall during winter and ablates during the summer. The climatic conditions of Himalaya vary with the mountain ranges or geographically which affects the snow metamorphism significantly. The western Himalaya can be divided in to three different snow climatic zones (Sharma and Ganju, 2000). The upper Himalayan zone is characterized by comparatively low temperatures, light snowfall and severe wind activities. The middle Himalayan zone is characterized by fairly cold temperatures, heavy and dry snowfall with strong wind action. The lower Himalayan zone is characterized by moderate temperatures, heavy snowfall and short winter period. The study of albedo and grain size can describe the snow metamorphism, snowmelt and regional climate of the Himalayan regions.

To retrieve the information of large snow cover extent from space-borne satellite sensors, it is important to understand the spectral signatures of different types of snow on ground because of the complex internal structure of snow and inhomogeneity in the snowpack (Massom et al., 2001). The advantages of field spectral measurements can be used in calibration of remote sensing sensors, predicting the optimum spectral bands for particular application, and development/testing of models relating to remote sensing data (Milton, 1987; Milton et al., 2009). Such systematic study provides the possibility of retrieving snow information from air-borne or space-borne sensors in different spectral regions as well as for the validation of satellite retrieved information.

In the present study reflectance measurements of different types of snow were measured at nadir viewing and attempts were made to retrieve snow properties i.e. snow albedo (plane, spherical and spectrally integrated) and snow grain size. The asymptotic radiative transfer (ART) theory was used for the different retrievals from snow signatures collected in lower Himalayan region. The selection of temperate region was because in this region one can get different types of metamorphosed snow signatures in a shorter duration to test the grain size retrieval models based on radiative transfer theory for snow, as the albedo reduction varies significantly for snow surface temperatures above $-10\,^{\circ}\mathrm{C}$ (Aoki et al., 2003).

TCD
4, 2337–2372, 2010

2 Field measurements

Reflectance measurements of Himalayan basin snow cover were carried out in field using ASD spectroradiometer in the spectral wavelength range of 350 nm–2500 nm with 3 nm spectral resolution in VIR and 10 nm spectral resolution at SWIR region. The reference surface used in the reflectance measurement was spectralon, a nearly perfect Lambertian reflector (Analytical Spectral Devices, 1999). To explore the ART theory for retrieving different parameters from spectral signatures of Himalayan snow, field experiments were made on seasonal fresh snow and old snow data with hourly temporal variations over a plane surface (Fig. 1). This investigation provided the different characteristics of snowpack such as new, old, dry, wet, homogeneous vs. inhomogeneous to explore the different analytical radiative transfer equations. All the experiments are carried out under clear sky conditions, i.e. direct solar radiation. The experiment was carried out within 5–10 min to minimize the atmospheric effect on snowpack. For fresh snow the field experiment was conducted on 29 January 2005, on day 1 after the cessation of snow storm, at latitude $32^\circ 16' 21''$ N and longitude $77^\circ 10' 58''$ E. This new snowfall was 10 cm on the top of existing snowpack and this set of reflectance measurements are termed as "Type-I snow". The old/metamorphosed snow reflectance measurements were carried out on 19 February 2008 at latitude $32^\circ 19' 03''$ N and longitude $77^\circ 09' 20''$ E. The previous snowfall that occured on existing snow buildup was only 3 cm and 4 days old. This set of observations is named as "Type-II snow" in the present study. The physical parameters measured at the time of field investigation are given in Table 1. The grain size was measured as average maximum grain diameter (EGD) using crystal gauge with magnifying hand lens. This method was found practical at the time of field investigations; although now advanced methods can be found in literature (e.g. Matzl and Schneebeli, 2006; Painter et al., 2007). The observations were carried out at nadir, i.e. viewing zenith angle was 0°.

Spectral albedo measurements were also carried out with each set of reflectance measurements to make the comparison with retrieved spectral albedo using ART

TCD
4, 2337–2372, 2010

theory (Kokhanovsky and Zege, 2004). The spectral albedo was measured using remote cosine receptor (RCR) connected to the spectroradiometer with fiber optic cable, by measuring downwelling irradiance followed by upwelling irradiance. Longer wavelengths (beyond 1800 nm) are removed from the spectrum due to very poor SNR of the measured spectral albedo. To validate the integrated albedo (i.e. using spectroradiometer) with broadband albedo (using field albedometer), we used another set of observations where we have both the measurements simultaneously for two days just after the snowfall. These experiments were made on 27 and 28 February 2006 in the same Himalayan basin at latitude 32°21′18″ N and longitude 77°07′35″ E.

3 ART theory

The remote sensing of snowpack was initially modeled by different researchers (Bohren and Barkstrom, 1974; Warren and Wiscombe, 1980; Warren, 1984) as a layer of dispersed spherical snow grains. The snow retrieval algorithms were made from reflectance characteristics for different satellite data using the model mentioned above (Nolin and Dozier, 1993; Fily et al., 1997; Hori et al., 2001; Li et al., 2001). This model uses Mie theory to obtain single scattering characteristics and radiative theory to relate radiative properties of snow to snow local optical characteristics.

However, snow on ground consists of irregularly shaped non uniform snow grains. The optical properties of snow not only controlled by size but also by the shape of the particles (Mishchenko et al., 1999, 2002; Kokhanovsky, 2003; Kokhanovsky and Zege, 2004). Therefore more realistic snow model with non-spherical snow grains are proposed by different researchers (Kokhanovsky and Zege, 2004; Zege et al., 2008) and retrievals were made using different satellite sensors (Kokhanovsky et al., 2005, 2011; Tedesco and Kokhanovsky, 2007; Lyapustin et al., 2009; Kokhanovsky and Schreier, 2009). In the present study, this approach has been considered, which introduce model of snow as fractal grains rather than spherical in order to account for their irregular shape, geometrical optics equations instead of Mie calculations for snow optical

TCD
4, 2337–2372, 2010

characteristics, and analytical asymptotic solutions of the radiative transfer theory for snow optical properties (Kokhanovsky and Zege, 2004). According to this theory snow reflection function can be modeled using approximate analytical solution in the form of the following equation valid for weakly absorbing snow layers (Kokhanovsky and Zege, 2004):

$$R(\mu,\mu_0,\varphi) = R_0(\mu,\mu_0,\varphi)A^{f(\mu,\mu_0,\varphi)}, \tag{1}$$

Here $R(\mu,\mu_0,\varphi)$ is reflectance of a semi infinite snow layer; $\mu_0=\cos\vartheta_0$; $\mu=\cos\vartheta$; ϑ_0, ϑ and φ are solar zenith, viewing zenith and relative azimuth angle, respectively. Also it follows:

$$A=\exp\left\{-4s/\sqrt{3}\right\} \text{ and } s=\sqrt{\frac{1-\omega_0}{1-g\omega_0}}, \tag{2}$$

Here, A is spherical snow albedo, ω_0 is the single scattering albedo and g is the asymmetry parameter. The function $f(\mu,\mu_0,\varphi)$ is given by the following ratio:

$$f(\mu,\mu_0,\varphi) = \frac{u(\mu_0)u(\mu)}{R_0(\mu,\mu_0,\varphi)}, \tag{3}$$

Function $u(\mu_0)$ is called the escape function. It determines the angular distribution of light escaping from the semi-infinite nonabsorbing media and can be approximately given by Kokhanovsky (2003):

$$u(\mu_0) = \frac{3}{7}(1 + 2\mu), \tag{4}$$

where R_0 is the reflection function of a semi-infinite snow layer under assumption that the single scattering albedo is equal to one, and R_0 can be calculated using, the Fourier components of the reflection function in the visible (for a nonabsorbing snow). These are tabulated using a code developed by Mishchenko et al. (1999). The code solves the Ambartsumian nonlinear integral equation for the harmonics $R^m(\mu,\mu_0)$ of the reflection

TCD

4, 2337–2372, 2010

Retrieval of snow albedo and grain size in Himalayan basin

H. S. Negi and A. Kokhanovsky

function. These harmonics can be stored in LUTs. Thus, the reflection function at any relative azimuth angle is found as:

$$R_0(\mu,\mu_0,\varphi) = R^0(\mu,\mu_0) + 2\sum_{m=1}^{M_{\max}} R^m(\mu,\mu_0)\cos(m\varphi), \tag{5}$$

Here $\mu = \cos\vartheta$ and the value of $M_{\max}$ is chosen from the condition that the next term does not contribute more than 0.01% in the sum (Eq. 5). Alternatively the function R_0 can also be calculated using approximation given by Kokhanovsky (2005):

$$R_0(\mu,\mu_0,\varphi) = \frac{A + B(\mu + \mu_0) + C\mu\mu_0 + p(\theta)}{4(\mu + \mu_0)}, \tag{6}$$

where $A = 1.247$, $B = 1.186$, $C = 5.157$, $p(\theta) = 11.1\exp(-0.087\theta) + 1.1\exp(-0.014\theta)$, θ is given in degrees and defined as $\theta = a\cos(-\mu\mu_0 + ss_0\cos\varphi)$.

The theoretical reflectance spectra for a semi-infinite turbid medium can be obtained by solving the nonlinear integral equation derived by Ambartsumian, using the invariance principles. However, such an approach is not suitable for the inverse problem solution, because of the computational burden (Kokhanovsky, 2006). Therefore, to make the faster retrievals the approximate relations have been used for spherical albedo, plane albedo, and grain size estimation.

4 Retrievals

The reflection function $R(\mu,\mu_0,\varphi,\varphi_0)$ is defined as the ratio of the intensity of light (upwelling radiance) reflected from a given turbid layer to the solar flux density reflected (direct irradiance) from the perfectly reflecting lambertian surface for a given incident beam direction and observation direction (Kokhanovsky, 2004a, 2006). Thus, R is determined by solar zenith angles ϑ_0, viewing angle ϑ, solar azimuth angle φ_0 and

TCD
4, 2337–2372, 2010

Retrieval of snow albedo and grain size in Himalayan basin

H. S. Negi and A. Kokhanovsky

viewing azimuth angle φ_1. R is equal to 1 for lambertian surface. Namely it follows:

$$R(\mu,\mu_0,\varphi_1,\varphi_0) = \frac{\pi L(\mu,\mu_0,\varphi_1,\varphi_0)}{\mu_0 E_d^{dir}(\mu_0,\varphi_0)}, \quad (7)$$

where, L is the upwelling radiance and E_d^{dir} is the incident direct irradiance. The reflectance measurements carried out during field investigation provide the above function, which was further used to make different retrievals.

4.1 Albedo

a. Plane albedo is also called as directional hemispherical reflectance and defined as the integral of reflectance function "R" over all reflection (viewing) angles, and can be derived from following equation:

$$r_p = \frac{1}{\pi}\int_0^{2\pi} d\varphi \int_0^1 R(\mu,\mu_0,\varphi)\mu d\mu, \quad (8)$$

where, μ is the cosine of viewing angle and φ is the relative azimuth angle.

b. Spherical albedo is also called as bi-hemispherical reflectance or diffuse albedo and defined as the integral of plane albedo "r_p" over all solar angles, and can be given by following equation:

$$r_s = 2\int_0^1 r_p(\mu_0)\mu_0 d\mu_0. \quad (9)$$

TCD
4, 2337–2372, 2010

c. Broadband albedo can be obtained by integrating the plane spectral albedo $r_p(\lambda)$ over the wavelength, weighted by the incident solar flux $F_{\downarrow}(\lambda)$:

$$a = \frac{\int r_p(\lambda)F_{\downarrow}(\lambda)d\lambda}{\int F_{\downarrow}(\lambda)d\lambda}. \tag{10}$$

The albedo defined by Eqs. (8) and (9) are not possible to determine from satellite sensors because measurements are performed with fixed solar and viewing angles. Kokhanovsky et al. (2007) presented an alternative possibility for direct determination of the spherical cloud albedo from single reflection function measurements, for the special case of optically thick cloudiness. This technique requires no a priori information on the particles size and optical thickness. It has also shown that the absolute value of error is below 3% at optical thickness $\tau \geq 10$ for all considered solar zenith angles and nadir observations, which is suitable in case of snow study.

From Eq. (1), using the ART theory, spherical albedo "A", can be retrieved from reflection measurements ($R_{\text{meas}} = R(\mu, \mu_0, \varphi)$) at a fixed geometry and can be given by following equation:

$$A = r_s = \left(\frac{R_{\text{meas}}}{R_0}\right)^{1/f}. \tag{11}$$

Thus spherical albedo can be retrived by substituting the value of f and R_0 from Eqs. (3) and (6), respectively. Once we know spherical albedo, the plane albedo can be determined by following relation (Kokhanovsky, 2002, 2004b):

$$r_p = A^{u(\mu_0)} \tag{12}$$

or

$$r_p = \left(\frac{R_{\text{meas}}}{R_0}\right)^{R_0/u(\mu)},$$

where, A and $u(\mu_0)$ can be substituted in Eq. (12) from Eqs. (11) and (4).

TCD
4, 2337–2372, 2010

Retrieval of snow albedo and grain size in Himalayan basin

H. S. Negi and A. Kokhanovsky

4.2 Grain size

The remote sensing provides the effective optical size of snow grains, which can be defined by average volume V and average projection area S of a snow grain, and can be represented as follows:

$$a_{\text{ef}} = \frac{3}{4}(V/S), \tag{13}$$

where V and S represent the particle volume and projected area, respectively (Jin et al., 2008; Kokhanovsky, 2011). In case of monodisperse spheres, the a_{ef} is the same as actual radius. It is a possible to determine a_{ef} using optical measurements on ground, aircraft or satellite (Dozier et al., 2009), since it has a physical sense, as the snow reflection function is governed mostly by the value of the probability of photon absorption (PPA) (Kokhanovsky et al., 2005). However, it is difficult to measure the a_{ef} with a microscope on ground, a lot of averaging procedures are to be required to derive the value of a_{ef} as given by Eq. (13). The other way to measure a_{ef} is the specific surface area (SSA), which can be measured by different direct techniques such as methane adsorption technique (Legagneux et al., 2002), microtomography (Schneebeli and Sokratov, 2004), near-infrared photography (Matzl and Scheebeli, 2006), and stereology (Matzl, 2006). The relation between SSA and a_{ef} is given by (Domine, 2008):

$$\text{SSA} = \frac{\overline{\Sigma}}{\rho_i \overline{V}}, \tag{14}$$

where ρ_i is the density of ice (0.9167 g cm^{-3}, at 0 °C) and $\overline{\Sigma}$, $\overline{V}$ are the averaged surface area and average volume with respect to the size/shape distributions of grains, respectively. In case of monodisperse spheres SSA can be defined as:

$$\text{SSA} = \frac{3}{\rho_i a_{\text{ef}}}. \tag{15}$$

Discussion Paper | Discussion Paper | Discussion Paper | Discussion Paper |
TCD
4, 2337–2372, 2010

Retrieval of snow albedo and grain size in Himalayan basin

H. S. Negi and A. Kokhanovsky

Therefore with the optical measurements of a_{ef}, one can also determine the SSA.

Different authors has used ART theory to retrieve grain size (Kokhanovsky and Zege, 2004a; Kokhanovsky and Nauss, 2005; Tedesco and Kokhanovsky, 2007; Kokhanovsky and Schreier, 2009). Now this theory has also been used by considering soot effect in NIR region in addition to ice absorption (Zege et al., 2008; Kokhanovsky, 2011) and as ratio techniques of different ice absorption channels (Lyapustin, 2009).

a. Single channel method: Kokhanovsky and Zege (2004) first defined the snow grain diameter (d) by physically based equation:

$$d = \frac{1}{\alpha b^2 f^2} \ln^2\left(\frac{R}{R_0}\right), \quad (16)$$

where $\alpha = 4\pi\chi(\lambda)/\lambda$ is the ice absorption coefficient, parameter b depends on the grain shape and asymmetry parameter (considered ≈3.62 for fractal particles; and ≈4.53 for spheres), R is the measured reflectance at NIR channel, and other terms are same as mentioned in Sect. 3. In the present study fractal particles are considered and R_0 is estimated using approximation method given by Eq. (6). Imaginary part of ice refractive index (χ) was used as tabulated by Warren and Brandt (2008).

b. Two channel method: Kokhanovsky et al. (2011), has proposed the two channel method to estimate the grain size and soot concentration using following equations:

$$R_1 = R_0 \exp(-\gamma\sqrt{\beta_1}) \quad (17)$$

$$R_2 = R_0 \exp(-\gamma\sqrt{\beta_2}) \quad (18)$$

where, R_1 and R_2 are the reflectance in visible and NIR channel. β_1 and β_2 are PPA in visible (i.e. 0.443 µm, light absorption due to soot presence) and NIR

(0.865/1.05/1.24 µm; light absorption due to ice and soot) channel respectively, and γ is given by:

$$\gamma = \frac{4f}{\sqrt{3(1-g\omega_0)}}. \tag{19}$$

In the present case, the difference of ω_0 from 1.0 in Eq. (19) was neglected. Solving the Eqs. (17) and (18) for the PPA due to ice $\beta_{i,2}$ in NIR channel (i.e. total PPA in NIR: β_2-PPA due to soot in NIR: $\beta_{s,2}$) to retrieve grain size:

$$\beta_{i,2} = \frac{\ln^2(R_2/R_0)}{\gamma^2} - \frac{\lambda_1}{\lambda_2}\left(\frac{\ln^2(R_1/R_0)}{\gamma^2}\right). \tag{20}$$

Subscript 1 and 2 denote the visible and NIR channel respectively, and imaginary part of refractive index for soot in visible and NIR channel is considered constant (0.46).

Finally, the effective grain radius was defined by Kokhanovsky and Nauss (2005):

$$a_{\mathrm{ef}} = (K\alpha_{i,2})^{-1}\ln\left[\frac{\beta_\infty}{\beta_\infty - \beta_{i,2}}\right], \tag{21}$$

where the value of $K = 2.63$ was considered in this study for fractals and $\alpha_{i,2}$ is a linear absorption coefficient for ice $\alpha = 4\pi\chi(\lambda)/\lambda$ in NIR channel. β_∞ is the limiting case of probability of photon absorption for an ice crystal, which absorbs all radiation penetrated inside the particle (considered $\beta_\infty = 0.47$), and $\beta_{i,2}$ can be substituted from Eq. (20).

Kokhanovsky et al. (2011) used LUTs approach, a code developed by Mishchenko et al. (1999) as discussed in Sect. 3 to estimate R_0, but presently we have used approximation method given by Eq. (6) so that the theory can be used to make fast snow retrievals using inversion technique.

TCD
4, 2337–2372, 2010

c. Two channel ratio method: Lyapustin et al. (2009) also used the ART theory given by Kokhanovsky and Zege (2004), instead of single band they used the band ratio method, where the role of R_0 reduced to the second order effect manifested in function "f". They defined the snow grain diameter (d) using two channels with different ice absorption by:

$$d = \frac{1}{4\pi b^2 f^2}\left[\ln\left(\frac{R_1}{R_2}\right)/(\sqrt{\chi_2/\lambda_2} - \sqrt{\chi_1/\lambda_1})\right]^2. \tag{22}$$

This equation is valid for vertically homogeneous snow. Here R1 and R2 are such that light penetration depth in snow are similar between the two wavelengths, and these can be selected as 1.05 and 1.24 µm. For inhomogeneous snow one ice non-absorbing channel (λ_1 in visible) and another ice absorbing channel (λ_2 in NIR) are required. In this case Eq. (22) can be given by:

$$d = \frac{\lambda_2}{4\pi\chi_2 b^2 f^2}\ln^2\left(\frac{R_1}{R_2}\right), \tag{23}$$

where R1 and R2 are the measured reflectance at visible and NIR channel, respectively. From Eqs. (16) and (23), it can be well observed that the difference is in the logarithmic part where R_0 is replaced with measured reflectance in visible channel. Lyapustin et al. (2009) has used the radiative transfer code for R_0, which is used to estimate "f" in Eq. (23). However in the present study, R_0 is again estimated from approximation method (Eq. 6). In this study the wavelength 0.645 µm is selected in the visible instead of 0.443 µm because the wavelength closed to channel 0.443 µm is more effected by contamination like soil/ash (Negi et al., 2009). Channels 0.645, 1.05 and 1.24 µm are used in the combination of (0.645 and 1.05 µm) and (0.645 and 1.24 µm).

d. Three channel method: Zege et al. (2008) defined new algorithm to retrieve snow grain size and pollution amount from satellite data using three channels

TCD
4, 2337–2372, 2010

reflectance measurement, with no priori snow optical model (i.e. for R_0). They defined effective size of snow grain by:

$$a_{\mathrm{ef}} = \left[\frac{1}{A(q_j - q_i)u(\mu_0)u(\mu)} \left(\frac{R_i^{q_j}}{R_j^{q_i}} \right)^{\frac{1}{q_j - q_i}} \ln\left(\frac{R_i}{R_j} \right) \right]^2, \tag{24}$$

where i and j are spectral channel, parameter A depends on shape of the particles and ranges from 3.5 to 6.5 (fractals to spheres; similar as denoted in Eq. (16) by "b") and q_i is given by:

$$q_i = \sqrt{4\pi \frac{(\chi_i + 0.2C_\mathrm{s})}{\lambda_i}}, \tag{25}$$

where C_s is relative soot concentration (i.e. soot and snow grain volumetric concentration), the detail analytical solution for estimating C_s is given by Eqs. (14–19) of Zege et al. (2008). There is one assumption that the effect of soot pollution on the light extinction in snow is zero. In the present study channels R2 (0.645 µm), R3 (0.859 µm), R4 (1.05 µm) and R5 (1.24 µm) are used in the combination of (R2, R3, R4) and (R2, R3, R5).

All the above discussed methods were used for the retrievals of snow grain size, and compared. In the present study the effective grain diameter "d" has been considered as retrieved snow grain size. Further by knowing the "d", spherical and plane albedo can be retrieved using approach described by Kokhanovsky and Zege (2004):

$$r_\mathrm{s} = \exp(-b\sqrt{\gamma d}), \tag{26}$$

and

$$r_\mathrm{p} = \exp(-u(\mu_0)b\sqrt{\gamma d}). \tag{27}$$

TCD
4, 2337–2372, 2010

H. S. Negi and A. Kokhanovsky

5 Field validation and discussions

5.1 Albedo

The plane and spherical albedo determined from temporal spectral reflectance measurement for Type-I and Type-II snow are shown in Figs. 2 and 3. The difference between the spectral reflectance and albedo is attributed to the presence of snow reflectance anisotropy, as the radiation reflected by snow surface is not distributed uniformly into all angles. An anisotropic reflection function (ARF), is defined by the ratio of reflectance to spectral albedo. It can be observed from the Fig. 2 (Type-I snow), the variation (ARF) in NIR region is throughout present (Fig. 2a to f), however in visible region this is varying with the solar zenith angle (SZA). As the SZA is decreasing with day time, the difference between reflectance and albedo is also decreasing in the visible region. In Fig. 2e, at low SZA, when Sun is around overhead (i.e. at 1150 h) the anisotropy is negligible in the visible region. For (Type-II snow), this anisotropy was observed along the whole spectrum i.e. visible and NIR region. The presence of anisotropy in the visible region could be explained by impurities in snow (e.g. clay/dust contamination and soot), as this anisotropy is consistent with respect to spherical albedo observations.

It has been observed that spherical albedo is lower than plane albedo for Fig. 2 (Type-I) and Fig. 3a–b (Type-II), and higher for Fig. 3d–e (Type-II). This difference between the plane and spherical albedo can be attributed by variation in albedo under diffuse radiation condition explained by Warren (1982), i.e. when SZA greater than 50° the spherical albedo (i.e. diffused albedo) decreases, however for SZA below 50°, the spherical albedo increases and remain unaltered around 50° (Wiscombe and Warren, 1980), which can be observed in case of Fig. 3c (SZA ∼48°).

The comparison between retrieved plane albedo and measured spectral albedo in field are shown by Fig. 4. It has been observed that the retrieved spectral albedo using ART theory is in good agreement with the measured spectral albedo in NIR region. The departures between retrieved and measured albedo in visible region are attributed to the measuring instrument response i.e. poor signal to noise (SNR) ratio in the visible region. Such difficulties during the measurement of spectral albedo in field under clear sky condition are also highlighted by other researchers (Warren, 1982; Warren et al., 1986; Aoki et al., 2000). However, the measurements were carried out over plane snow surface and leveling of the sensor has been taken care during the observations. Secondly in Fig. 4a–c, the measured spectral albedo in the visible region should not decrease being for a new snow (Type-I). The comparison of retrieved temporal albedo for snow Type-I and Type-II shows an agreement within 10% error in measured albedo at wavelength 1.05 µm and 1.24 µm (Fig. 5).

The integrated albedo was estimated using direct measurement of spectral albedo (i.e. using RCR) and retrieved plane albedo (using above theory), and compared with direct broadband albedo measurements (Fig. 6). Figure 6a and b show that integrated albedo data from spectroradiometer (direct and retrieved from reflectance) are close to broadband data. Generally all the integrated albedo using direct measurement having slightly less values than retrieved integrated albedo from reflectance data, this also proves the systematic error in our measured spectral albedo data in the visible region. The retrieved integrated albedo was found within ±6% difference error from ground observed broadband albedo. The coefficient of correlation between broadband and integrated albedo using spectral measurements was 0.89 with standard error (SE) 0.028 (Fig. 7a), however it was improved for intergrated retrieved albedo using reflectance i.e. 0.94 with SE 0.020 (Fig. 7b). This indicate that albedo retrievel form reflectance using ART theory can work well for Himalayan snow.

5.2 Grain size

The field reflectance measurement data in R1(443 nm), R2(645 nm), R3(859 nm), R4(1050 nm) and R5(1240 nm) channels for retrieving grain sizes by different models are given by Fig. 8a and b for snow Type-I and Type-II, respectively. A slight variation in reflectance can be observed in R1, R2 and R3 channels due to variations in atmospheric and snow conditions with time under natural field environment but for R4 and R5 decreasing trend was observed which is attributed to increasing trend of snow grain size. Field measured parameters (Table 1) also indicate temporal increasing in grain size for both types of snow, as the snow grain size increases due to clustering of snow grains at snow temperature close to 0 °C (Colbeck, 1982). For snow Type-II, the reflectances at R5(1240 nm) are less than 0.2, where the ART theory fails as the theory is only valid for semi infinite media with low absorption (Kokhanovsky and Zege, 2004) and therefore grain size was not retrieved for such low reflectances.

The grain size retrievals were made using four methods as discussed in Sect. 4.2, and shown by Table 2. The retrieved grain size for snow Type-I were underestimated compared to ground measured snow grain sizes in first three methods, this suggests that the ground measured grain size i.e. maximum equivalent grain diameter of is not a correct measure. Aoki et al. (2000) also reported after observing three types of grain equivalent measurements on ground and found that effective grain size falls in the range of measured lengths of narrower portions of broken crystals. Unfortunately we could not make such fine level length measurements using field instruments available to us for new snow, however as the snow become rounded due to metamorphism, the retrieved grain sizes are in agreement with measured one (snow Type-II). The three channel method retrieved larger grain sizes and found to be much more sensitive to difference between reflectance observed in visible and NIR region. Since in this method one additional NIR channel R3 was used so we are not considering this method to compare with other models where only one NIR channel was used to retrieve the grain sizes.

From Table 2 and Fig. 9, a good agreement can be observed between retrieved grain sizes with temporal increment using the single channel method and two channel method. However, slight variation was observed using two channel ratio method. All the three methods retrieved almost similar grain sizes once the snow was new (snow type-I) with very fine grain and dry (snow surface temperature less than 0 °C). However, two channel ratio method retrieved smaller grain size as compared to two channel method once the snow metamorphosed (snow Type-II). This difference in retrieved

TCD
4, 2337–2372, 2010

grain sizes from other two methods attributed to replacement of R_0 by visible channel reflectance (R2), where a large difference can be observed between R_0 and measured R2. The deviation in retrieved grain sizes using three channel method with grain sizes retrieved from other methods may be due to the exclusion of R_0 using visible channel. Therefore the two channel ratio method or three channel method can work well for the snow covered area where the visible channel reflectance is high, like in Polar Regions or upper Himalaya but not for lower and middle Himalayan seasonal snow due to higher temperature and proximity to habitat area. The single channel method and two channel method have similar grain size trend with slight difference in sizes derived from 1.05 µm for snow Type-I and Type-II (Fig. 9). This difference is due to soot effect at 1.05 µm, which can be observed negligible for channel 1.24 µm. Secondly it was found that the grain sizes derived using two channel method are more close to the ground measured grain diameter, in comparison to grain size derived from single channel method. Therefore we propose two channel method for various type of Himalayan seasonal snow.

Retrieved grain sizes using channel 1.05 µm and 1.24 µm for snow Type-I, using all the methods showed a linear relations for small grain sizes i.e. early hours of the day (Fig. 10). However, this deviation is more for larger grain sizes i.e. with respect to time, which indicate the presence of vertical inhomogeneity in the snowpack at late hours of the day, as wavelength 1.05 µm penetrates more in snow than that at 1.24 µm. Ground snow cover information also supports the vertical inhomogeneity at later day time as the fresh snowfall produced only 10 cm of snow on existed snowpack, which become thin by the later hours and thus the variation in retrieved grain sizes was observed due to underlying old snow with different grain sizes.

Further, the spherical and plane albedos can also be modeled using ART theory once the effective grain diameter "*d*" was correctly estimated. The theoretical spherical albedo and the retrieved spherical albedo from reflectance measurement for snow Type-I was observed well in agreement up to 1400 nm and for larger wavelength error increased due to limitation of theory for large absorption (Fig. 11). But such good agreement between theoretical albedo and retrieved albedo can not be observed for snow Type-II, as the low reflectances in visible region cause lower actual albedo. Therefore one can retrieve the albedo from single channel in NIR using ART theory for clean snow but we suggest for the Himalayan-like seasonal snow the narrow band to broadband (NTB) albedo can work well for albedo estimation from the space, where NTB albedo can be retrieved from reflectance as discussed in Sects. 4.1. and 5.1.

6 Conclusions

The main advantage of the ART theory is analytical solutions of the radiative transfer theory for retrieving the snow properties. This makes the fast retrievals instead of running radiative transfer codes. Therefore this technique can be used to generate the operational snowcover grain size and albedo maps using airborne or spaceborne mutispectral sensor data. Before directly applying the theory to retrieve the snow properties from satellite data of Himalayan region, it was an important step to understand how it behaves for the different types of seasonal snow.

With this study, it was found that the ART theory can work well for retrieving seasonal snow albedo (i.e. plane and spherical). This is also an important input for retrieving narrow band to broadband albedo. The comparison of retrieved grain sizes using different models for different type of snow helped in understanding the advantage and limitations of these methods for Himalayan region. The two channel method was found suitable for all the type of snow studied, this method can use any NIR channel (0.865/1.05/1.24 µm) as it can take care of absorption in NIR channel due to soot. The other grain size methods using directly visible channel reflectance for R_0 to retrieve grain sizes are found sensitive to visible snow reflectance and such models are inconsistent for retrieving the grain sizes. The detection of vertical inhomogenety within the snowpack using grain retrievals by different ice absorption channels can be very helpful in snow avalanche study of Himalayan region to find the stability of the snowpack.

Acknowledgements. H. S. Negi thanks to Department of Science and Technology (DST), India for providing BOYSCAST fellowship to this work, and Snow & Avalanche Study Establishment (SASE), DRDO, India for supporting to carry out this study and all the field investigations. A. Kokhanovsky thanks ESA (Snow-Radiance Project) and JAXA (SGLI Cryosphere Project) for support of this research. He also acknowledges the support of the BMBF Project CLIMSLIP. The authors are grateful to J. B. Burrows, IUP, University of Bremen, Germany and A. V. Kulkarni, IISc. Bangalore, India for support and discussions.

References

Analytical Spectral Devices: Fieldspec TM, Technical Guide, 3rd edn., Boulder, Co, USA, 1999.

Aoki, T., Aoki, T., Fukabori, M., Hachikubo, A., Tachibana, Y., and Nishio, F.: Effects of snow physical parameters on spectral albedo and bi-directional reflectance of snow surface, J. Geophys. Res., 105(D8), 10219–10236, 2000.

Aoki, T., Hachikubo, A., and Hori, M.: Effects of snow physical parameters on shortwave broadband albedos, J. Geophys. Res., 108(D19), 4616, doi:10.1029/2003JD003506, 2003.

Bohren, C. F. and Barkstrom, B. R.: Theory of the optical properties of snow, J. Geophys. Res., 79(30), 4527–4535, 1974.

Colbeck, S. C.: An overview of seasonal snow metamorphism, Rev. Geophys. Space Ge., 20, 45–61, 1982.

Domine, F., Albert, M., Huthwelker, T., Jacobi, H.-W., Kokhanovsky, A. A., Lehning, M., Picard, G., and Simpson, W. R.: Snow physics as relevant to snow photochemistry, Atmos. Chem. Phys., 8, 171–208, doi:10.5194/acp-8-171-2008, 2008.

Dozier, J., Green, R. O., Nolin, A. W., and Painter, T. H.: Interpretation of snow properties from imaging spectrometry, Remote Sens. Environ., 113, S25–S37, 2009.

Fily, M., Bourdelles, B., Dedieu, J. P., and Sergent, C.: Comparison of in situ and Landsat thematic mapper derived snow grain characteristics in the Alps, Remote Sens. Environ., 59, 452–460, 1997.

Hori, M., Aoki, T., Stamnes, K., Chen, B., and Li, W.: Preliminary validation of the GLI cryosphere algorithms with MODIS daytime data, Polar Met. Glacio., 15, 1–20, 2001.

Jin, Z., Charlock, T. P., Yang, P., Xie, Y., and Miller, W.: Snow optical properties for different

particle shapes with application to snow grain size retrieval and MODIS/CERES radiance comparison over Antarctica, Remote Sens. Environ., 112, 3563–3581, 2008.
Li, W., Stamnes, K., Chen, B., and Xiong, X.: Snow grain size retrieved from near-infrared radiances at multiple wavelengths, Geophy. Res. Lett., 28, 1699–1702, 2001.
Kokhanovsky, A. A.: Statistical properties of a photon gas in random media, Phys. Rev., E66, 1–4, 2002.
Kokhanovsky, A. A.: Polarization optics of random media, Springer, Dordrecht, UK, 2003.
Kokhanovsky, A. A., Rozanov, V. V., Zege, E. P., Bovensmann, H., and Burrows, J. P.: A semi-analytical cloud retrieval algorithm using backscattering radiation in 04.–2.4 µm spectral range, J. Geophy. Res., 108(D1), 1–19, 2003.
Kokhanovsky, A. A. and Zege, E. P.: Scattering optics of snow, Appl. Optics, 43(7), 1589–1602, 2004.
Kokhanovsky, A. A.: Cloud optics, Springer-Praxis, Chichester, Netherlands, 2004a.
Kokhanovsky, A. A.: Spectral reflectance of whitecaps, J. Geophy. Res., 109, C05021, doi:10.1029/2003JC002177, 2004b.
Kokhanovsky, A. A.: Reflection of light from a semi-infinite medium with irregularly shaped particles, J. Quant. Spectrosc. Ra., 96, 1–10, 2005.
Kokhanovsky, A. A. and Nauss, T.: Satellite based retrieval of ice cloud properties using semi-analytical algorithm, J. Geophy. Res., 110, D19206, doi:10.1029/2004JD005744, 2005.
Kokhanovsky, A. A., Aoki, T., Hachikubo, A., Hori, M., and Zege, E. P.: Reflective properties of natural snow: approximate asymptotic theory versus in situ measurements, IEEE T. Geosci. Remote, 43(7), 1529–1535, 2005.
Kokhanovsky, A. and Sokoletsky, L. G.: Reflection of light from semi-infinite absorbing turbid media, part 1: spherical albedo, Color Res. Appl., 31(6), 491–497, 2006.
Kokhanovsky, A., Mayer, B., von Hoyningen-Huene, W., Schmidt, S., and Pilewskie, P.: Retrieval of cloud spherical albedo from top-of-atmosphere reflectance measurements performed at a single observation angle, Atmos. Chem. Phys., 7, 3633–3637, doi:10.5194/acp-7-3633-2007, 2007.
Kokhanovsky, A. and Schreier, M.: The determination of snow specific surface area, albedo and effective grain size using AATSR space-borne measurements, Int. J. Remote Sens., 30(4), 919–933, 2009.
Kokhanovsky, A. A., Rozanov, V. V., Aoki, T., Odermatt, D., Brockmann, B., Kruger, O., Bouvet, M., Drusch, M., and Hori, M.: Sizing snow grains using backscattered solar light, Int. J.

TCD
4, 2337–2372, 2010

Retrieval of snow albedo and grain size in Himalayan basin

H. S. Negi and A. Kokhanovsky

Remote Sens., in press, 2011.
Legagneux, L., Cabanes, A., and Domine, F.: Measurement of the specific surface area of 176 snow samples using methane adsorption at 77 K, J. Geophys. Res., 107(D17), 4335, doi:10.1029/2001JD001016, 2002.
Lyapustin, A., Tedesco, M., Wang, Y., Aoki, T., Hori, M., and Kokhanovsky, A.: Retrieval of snow grain size over Greenland from MODIS, Remote Sens. Environ., 113, 1976–1987, 2009.
Massom, R. A., Eicken, H., Haas, C., Jeffris, M. O., Drinkwater, M. R., Sturm, M., Worby, A. P., Wu, X., Lytle, V. I., Ushio, S., Morris, K., Reid, P. A., Warren, S. G., and Allison, I.: Snow on Antarctic ice, Rev. Geophys., 39, 413–445, 2001.
Matzl, M.: Quantifying the stratigraphy of snow profiles, Ph.D thesis, Swiss Federal Institute of Technology, Zurich, 2006.
Matzl, M. and Schneebelli, M.: Measuring specific surface area of snow by near-infraref photography, J. Glaciol., 52(179), 558–564, 2006.
Milton, E. J.: Principles of field spectroscopy-Review Article, Int. J. Remote Sens., 8(12), 1807–1827, 1987.
Milton, E. J., Schaepman, M. E., Anderson, K., Kneubühler, M., and Fox, N.: Progress in field spectroscopy, Remote Sens. Environ., 113, 92–109, 2009.
Mishchenko, M. I., Dlugach, J. M., Yanovitskij, E. G., and Zakharova, N. T.: Bidirectional reflectance of flat, optically thick particulate layers: an efficient radiative transfer solution and applications to snow and soil surfaces, J. Quant. Spectrosc. Ra., 63, 409–432, 1999.
Mishchenko, M. I., Travis, L. D., and Lacis, A. A.: Absorption, scattering, and emission of light by small particles, Cambridge U. Press, Cambridge, 2002.
Negi, H. S., Kulkarni, A. V., and Semwal, B. S.: Study of contaminated and mixed objects snow reflectance in Indian Himalaya using spectroradiometer, Int. J. Remote Sens., 30(2), 315–325, 2009.
Nolin, A. W. and Dozier, J.: Estimating snow grain size using AVIRIS data, Remote Sens. Environ., 44, 231–238, 1993.
Painter, T. H., Molotch, N. P., Cassidy, M., Flanner, M., and Steffen, K.: Instruments and methods contact spectroscopy for determination of stratigraphy of snow optical grain size, J. Glaciol., 53(180), 121–127, 2007.
Schneebeli, M. and Sokratov, S. A.: Tomography of temperature gradient metamorphism of snow and associated changes in heat conductivity, Hydrol. Process., 18, 3655–3665, 2004.
Sharma, S. S. and Ganju, A.: Complexities of avalanche forecasting in Western Himalaya – an

overview, Cold Reg. Sci. Technol., 31, 95–102, 2000.
Tedesco, M. and Kokhanovsky, A. A.: The semi-analytical snow retrieval algorithm and its application to MODIS data, Remote Sens. Environ., 110, 317–331, 2007.
Zege, E., Katsev, I., Malinka, A., Prikhach, A., and Polonsky, I.: New algorithm to retrieve the effective snow grain size and pollution amount from satellite data, Ann. Glaciol., 49, 139–144, 2008.
Warren, S. G. and Wiscombe, W. J.: A model for the spectral albedo of snow-II: snow containing atmospheric aerosols, J. Atmos. Sci., 37, 2734–2745, 1980.
Warren, S. G.: Optical properties of snow, Rev. Geophys. Space Ge., 20(1), 67–89, 1982.
Warren, S. G., Grenfell, T. C., and Mullen, P. C.: Optical properties of Antarctic snow, Antarct. J. US, 21, 247–248, 1986.
Warren, S. G. and Brandt, R. E.: Optical constant of ice from the ultraviolet to the microwave: A revised compilation, J. Geophy. Res., 113, D114220, doi:10.1029/2007JD009744, 2008.
Wiscombe, W. J. and Warren, S. G.: A model for the spectral albedo of snow-I: pure snow, J. Atmos. Sci., 37, 2712–2733, 1980.

TCD
4, 2337–2372, 2010

Table 1. Field measured snow parameters at the time of reflectance observations (Not meas. is no measurement recorded).

Snow type and date	Time (LT)	Solar zenith angle (degree)	Snow thickness (cm)	Snow surface temperature (°C)	Grain size (mm)
Type-I 29 January 2005	09:30	63.9	27	−2.0	0.0–0.5
	10:20	57.6	27	−2.0	0.0–0.5
	10:45	54.9	26	−1.5	0.5–1.0
	11:20	52.2	24	0.0	0.5–1.0
	11:50	51.0	23	0.0	1.0–2.0
	12:20	50.7	22	0.0	1.0–2.0
Type-II 19 February 2008	09:20	60.9	136	−1.0	1.0–2.0
	10:10	53.5	Not meas.	−0.5	1.0–2.0
	11:00	47.9	Not meas.	0.0	1.0–2.0
	12:00	44.6	Not meas.	0.0	1.0–2.0
	13:00	45.8	Not meas.	0.0	1.0–2.0

TCD
4, 2337–2372, 2010

Retrieval of snow albedo and grain size in Himalayan basin

H. S. Negi and A. Kokhanovsky

Table 2. Retrieved snow grain size "*d*" (i.e. $2 \times a_{ef}$) using single channel method, two channel method, two channel ratio method and three channel method: R1, R2, R3, R4 and R5 are the reflectance at channel 0.443, 0.645, 0.859, 1.05 and 1.24 µm, respectively.

Snow type and date of observation	Time of observation	Grain size (mm) using single channel method		Grain size (mm) using two channel method		Grain size (mm) using two channel Ratio method		Grain size (mm) using three channel method	
	(LT)	R4	R5	R1, R4	R1, R5	R2, R4	R2, R5	R2, R3, R4	R2, R3, R5
Type-I 29 January 2005	09:30	0.14	0.15	0.14	0.14	0.12	0.14	0.33	0.37
	10:20	0.17	0.15	0.16	0.15	0.11	0.13	0.35	0.30
	10:45	0.28	0.32	0.27	0.31	0.22	0.29	0.94	0.87
	11:20	0.36	0.34	0.35	0.33	0.23	0.28	0.72	0.65
	11:50	0.48	0.52	0.45	0.51	0.34	0.45	1.07	1.14
	12:20	0.81	0.89	0.76	0.91	0.43	0.69	1.34	1.80
Type-II 19 February 2008	09:20	1.81	–	1.70	–	0.69	–	1.64	–
	10:10	1.80	–	1.66	–	0.66	–	1.67	–
	11:00	2.04	–	1.91	–	0.85	–	2.28	–
	12:00	2.11	–	1.96	–	0.84	–	2.26	–
	13:00	2.07	–	1.95	–	0.94	–	2.43	–

TCD
4, 2337–2372, 2010

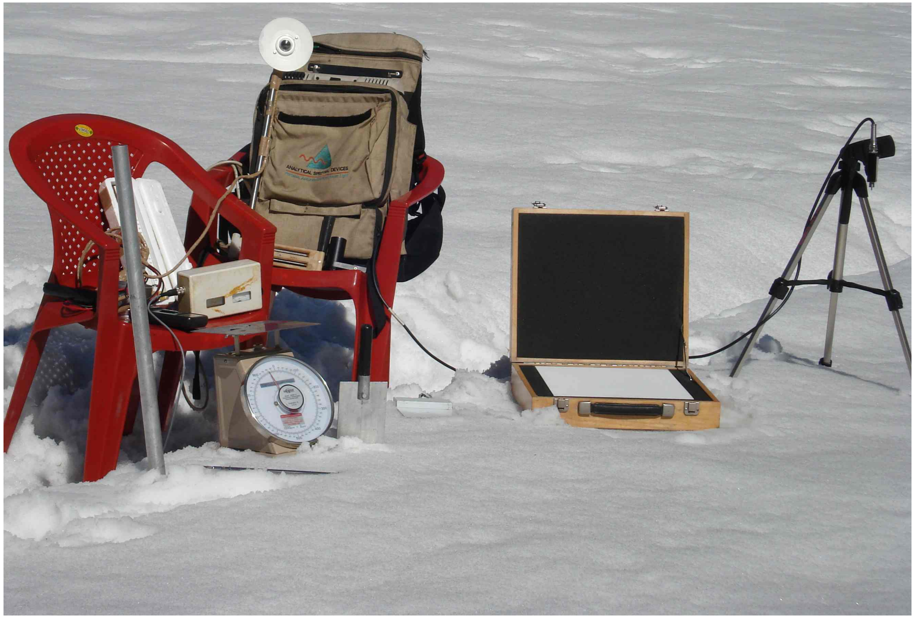

Fig. 1. Field experiment set-up of spectral reflectance measurements (winter 2008).

TCD

4, 2337–2372, 2010

Retrieval of snow albedo and grain size in Himalayan basin

H. S. Negi and A. Kokhanovsky

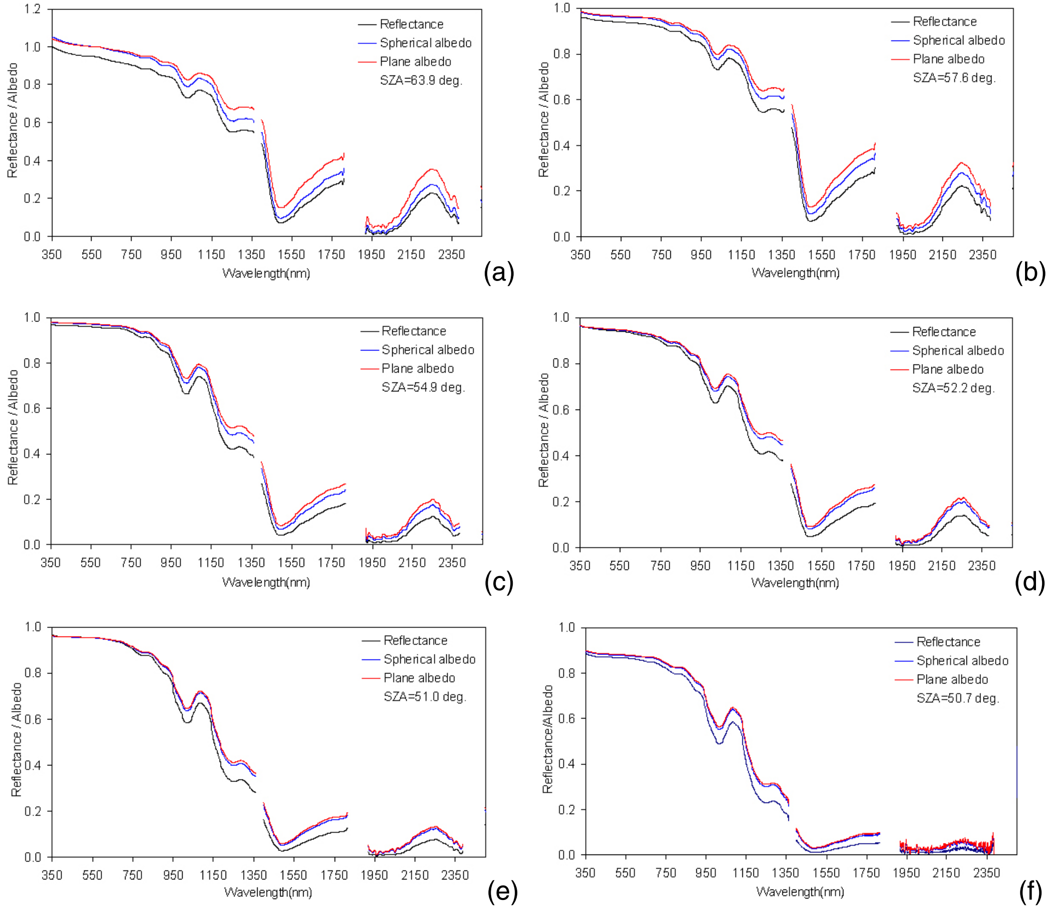

Fig. 2. Field measured reflectance for new snow and retrieved spherical and plane albedo; **(a)** 09:30, **(b)** 10:20, **(c)** 10:45, **(d)** 11:20, **(e)** 11:50 and **(f)** 12:20 local time.

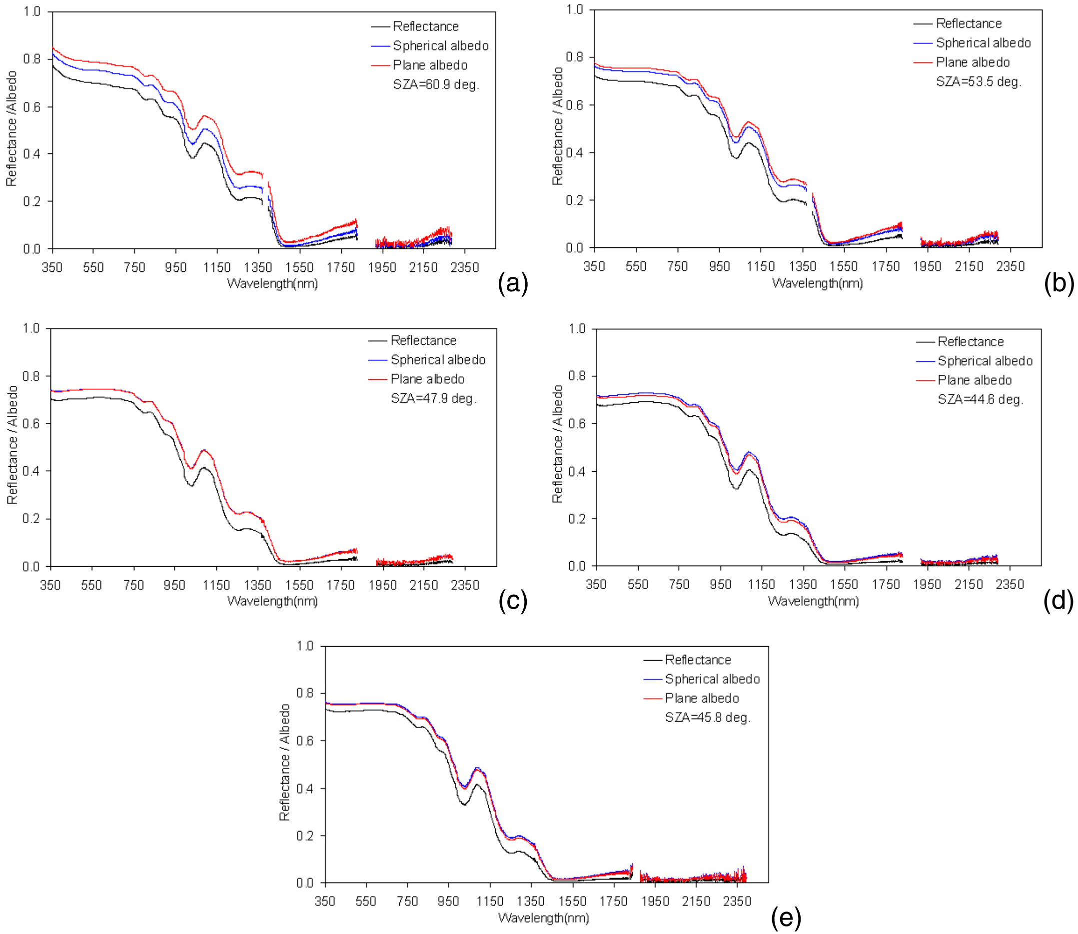

Fig. 3. Field measured reflectance for old snow and retrieved spherical and plane albedo; **(a)** 09:20, **(b)** 10:10, **(c)** 11:00, **(d)** 12:00 and **(e)** 13:00 local time.

TCD
4, 2337–2372, 2010

Title Page
Abstract | Introduction
Conclusions | References
Tables | Figures
◀I | ▶I
◀ | ▶
Back | Close
Full Screen / Esc
Printer-friendly Version
Interactive Discussion

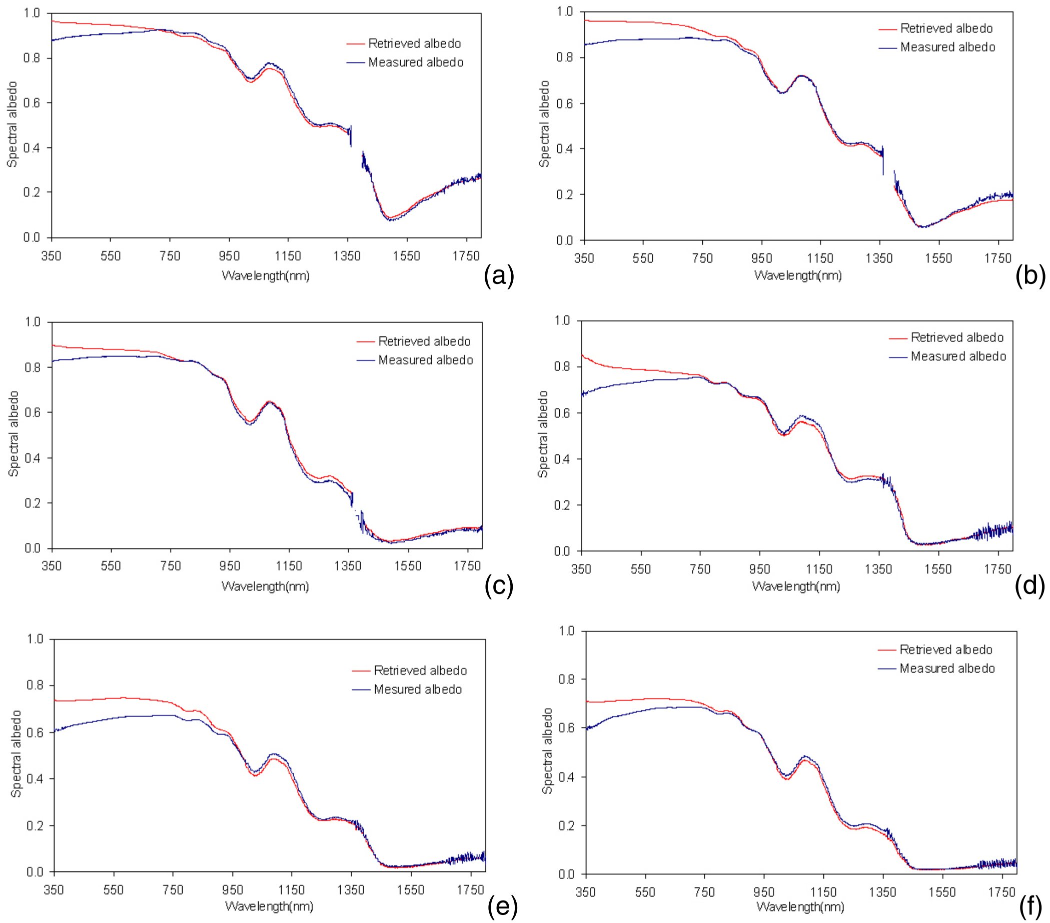

Fig. 4. Comparison of retrieved plane albedo with field measured spectral albedo; **(a)**–**(c)** are for snow Type-I at 11:20, 11:50 and 12:20 local time, and **(d)**–**(f)** are for snow Type-II at 09:20, 11:00 and 12:00 local time, respectively.

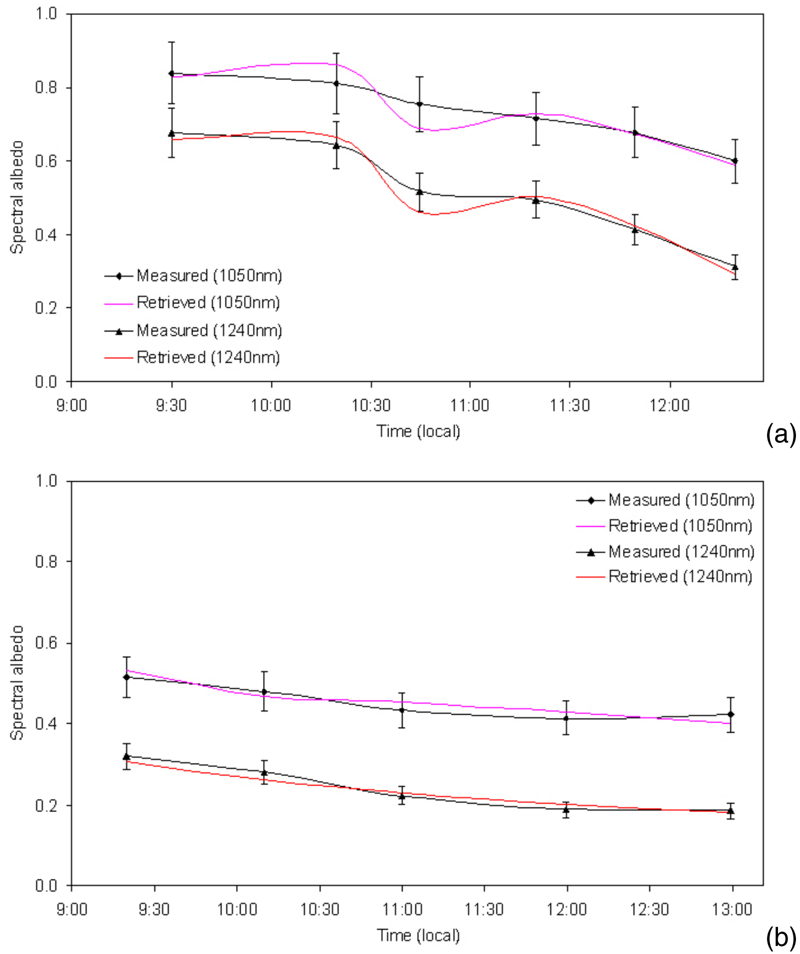

Fig. 5. Comparison of retrieved temporal albedo with measured spectral albedo with 10% measurement error at wavelength 1.05 µm and 1.24 µm for **(a)** snow Type-I and **(b)** Type-II.

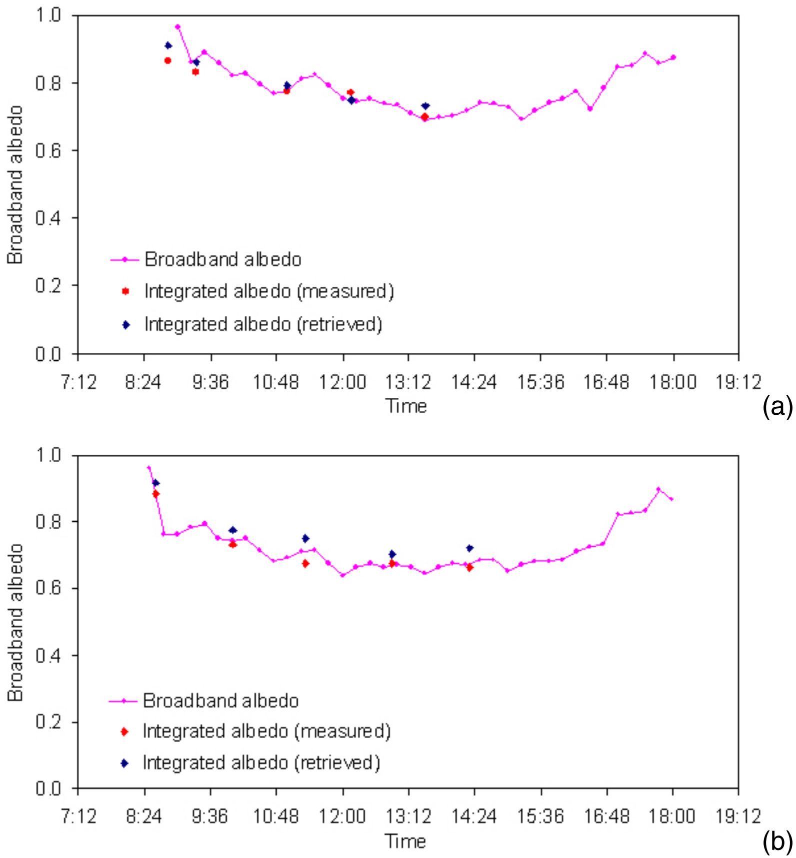

Fig. 6. Comparison between integrated albedo (measured and retrieved) with observed broadband albedo: **(a)** day 1 after snowfall 27 Feburary 2006, **(b)** day 2 after snowfall 28 February 2006.

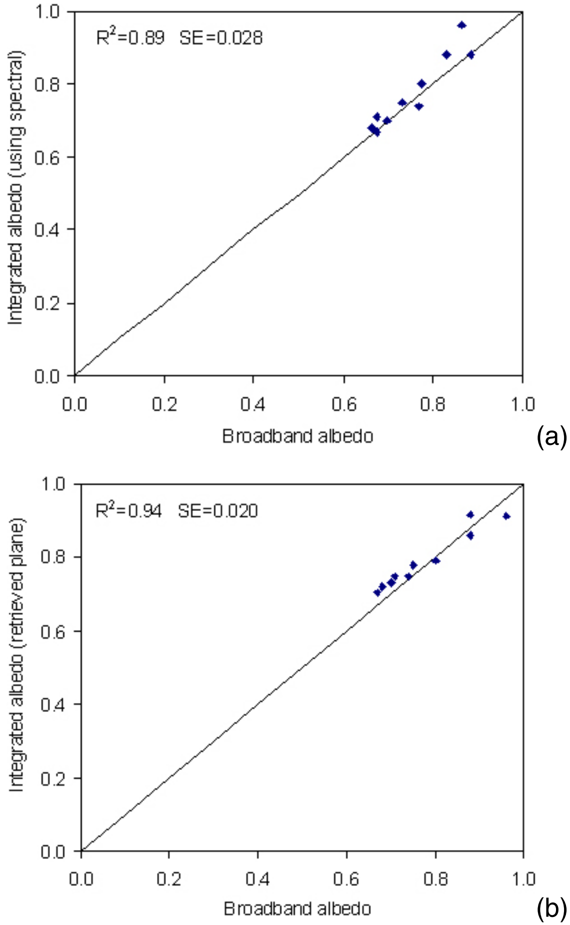

Fig. 7. Comparison between **(a)** broadband albedo and integrated albedo (using field measured spectral albedo); **(b)** broadband albedo and integrated albedo (using plane albedo retrieved from reflectance measurement data).

TCD

4, 2337–2372, 2010

Title Page
Abstract | Introduction
Conclusions | References
Tables | Figures
◀| |▶
◀ ▶
Back | Close
Full Screen / Esc
Printer-friendly Version
Interactive Discussion

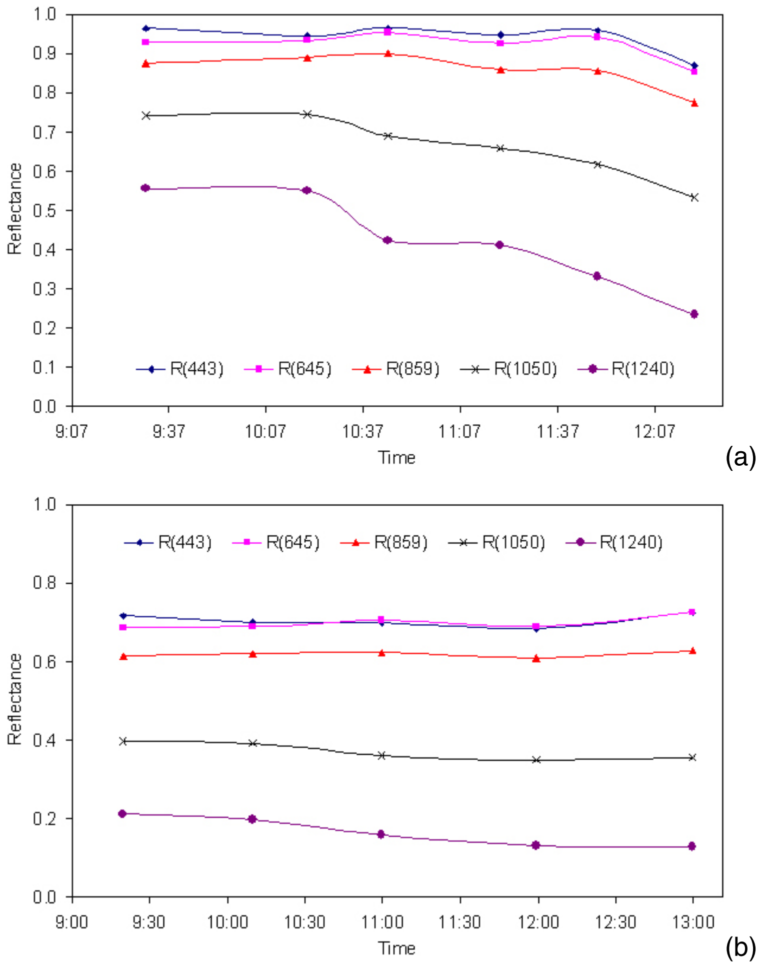

Fig. 8. Field measured reflectances of snow at wavelength 443, 645, 859, 1050 and 1240 nm **(a)** snow Type-I and **(b)** snow Type-II.

TCD
4, 2337–2372, 2010

Retrieval of snow albedo and grain size in Himalayan basin

H. S. Negi and A. Kokhanovsky

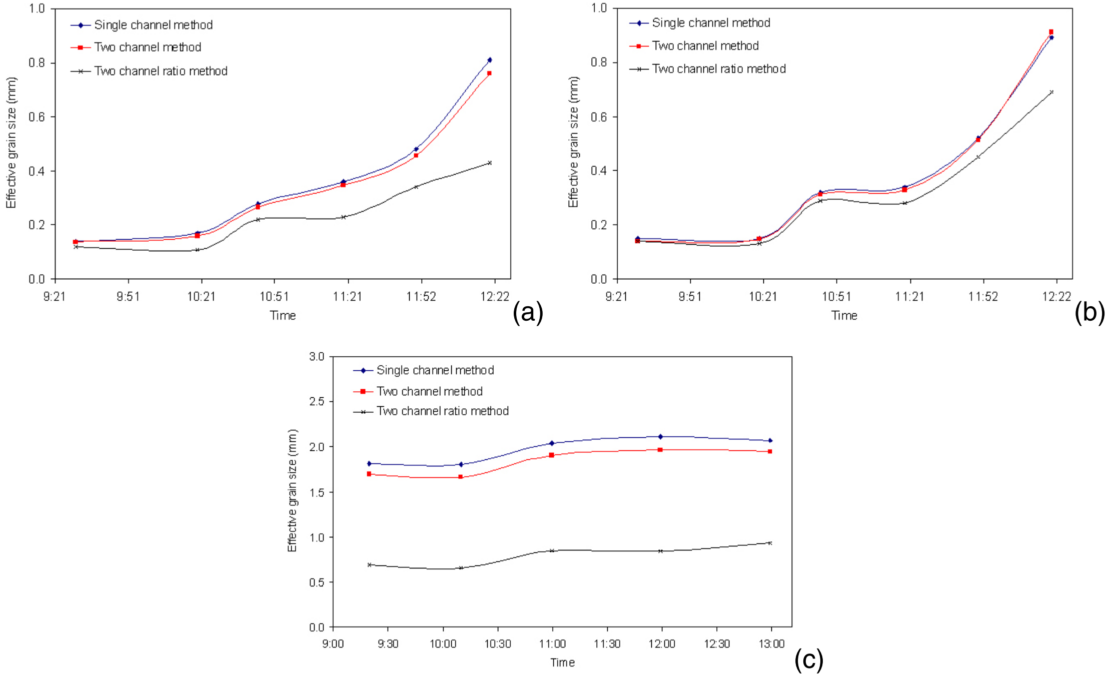

Fig. 9. Comparison of retrieved snow grain sizes; **(a)** snow Type-I using 1050 nm channel; **(b)** snow Type-I using 1240 nm channel and **(c)** snow Type-II using 1050 nm channel.

TCD
4, 2337–2372, 2010

Retrieval of snow albedo and grain size in Himalayan basin

H. S. Negi and A. Kokhanovsky

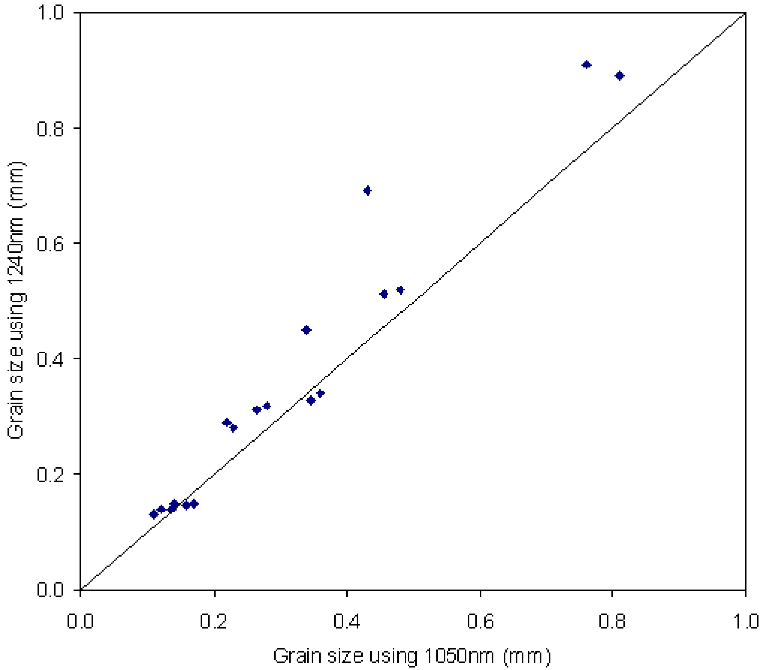

Fig. 10. Retrieved grain sizes using channel 1050 and 1240 nm for snow Type-I.

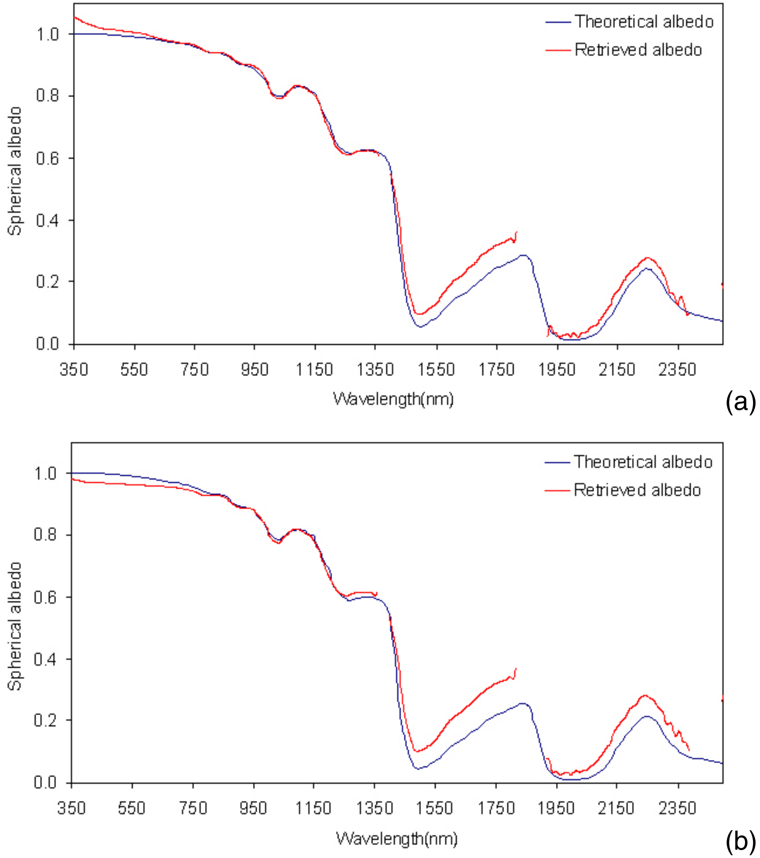

Fig. 11. Comparison between theoretical spherical albedo using ART (grain size from two channel model) and retrieved spherical albedo from the measured reflectance for snow Type-I **(a)** 09:30 and **(b)** 10:20 local time.